New Monolayer Architecture Constructed by Competitive Hydrogen-Bonding Force and Compression Pressure Characterized by Infrared Multiple-Angle Incidence Resolution Spectroscopy

Takeshi Hasegawa,*,† Junzo Umemura,‡ Changqing Li,§ and Roger M. Leblanc§

Department of Applied Molecular Chemistry, College of Industrial Technology, Nihon University, 1-2-1 Izumi-cho, Narashino, Chiba 275-8575, Japan, Institute for Chemical Research, Kyoto University, Gokasho, Uji, Kyoto-fu 611-0011, Japan, and Department of Chemistry, University of Miami, P.O. Box 249118, Coral Gables, Florida 33124-0431

Received: July 11, 2003; In Final Form: September 2, 2003

A unique monolayer that has a novel film architecture has been constructed by controlling a balance of hydrogen-bonding force and monolayer compression pressure, and the new film architecture has been characterized by infrared multiple-angle incidence resolution spectroscopy (MAIRS) that has recently been developed. The compound synthesized for the study consists of a single hydrocarbon chain and a headgroup that has three trans amide moieties. The limiting molecular area of the monolayer isotherm was approximately double that typically obtained for a single alkanoic-acid chain molecule, which suggested unusual film architecture. Then, the monolayer was transferred on a germanium substrate by the Langmuir−Blodgett film technique, and it was subjected to the infrared MAIRS analysis. The in-plane and out-of-plane mode spectra of MAIRS clearly suggested a flat alignment of interdigitated hydrogen-bonding networks and standing hydrocarbon chains with a disordered kink, which were totally consistent with a corresponding infrared reflection−absorption spectrum and the results of the isotherm measurement. The study suggests that the strongly correlated physical parameters are useful to develop a new film architecture.

Introduction

Monolayer films on water assembled by the Langmuir technique and transferred films on a solid substrate by the Langmuir−Blodgett (LB) film technique[1] have a unique characteristic that the molecules in the film are packed in a high density by high compression pressure. The degree of monolayer compression corresponds to "surface pressure" measured in a unit of mN m^{-1}, which has the same dimension as that of surface tension. Although this unit is convenient as a measure of film molecular compression, it is a little far from our general sense of "pressure". Let us then consider what pressure is applied to the monolayer,[2] when a monolayer of stearic acid is compressed on water up to 30 mN m^{-1}, for example. At the surface pressure of 30 mN m^{-1}, the monolayer is known to be in the solid state, which results in a thickness of 2.5 nm. Therefore, the pressure applied to the cross-section (perpendicular to the monolayer surface) of the monolayer in a width of one meter is calculated to be 12 MPa which corresponds to 118 atm. In this manner, a surface monolayer in the solid (or condensed) state is found to have a unique field, in which a considerably high pressure is applied to the spread molecules to form a two-dimensional crystal.

The extraordinary high pressure generated in the in-plane direction is a promisingly important physical parameter in terms of constructing unique film architecture. In a conventional way of preparation of monolayer films, hydrophobic interaction among the monomer molecules[3] and hydrogen bonding[4] are major key parameters to elucidate the film architecture. In our recent reports, however, a force balance between more physical parameters including compression pressure has positively been used to create novel film architectures.[5−7]

One of the former studies was regarding the "architecture switching" by film-to-film junction via surface pressure control.[5] This study was performed by use of two amphiphilic compounds that are barbituric acid (BA) and triaminotriazine (TAZ) derivatives. BA and TAZ moieties are very well known to form a multipoint hydrogen-bonding coupling,[8,9] which is often used as functional groups for strong molecular recognition. In our study, two monolayers of the BA and TAZ derivatives were individually prepared, and they were directly overlaid with each other at different surface pressures by the LB film technique. As a result, two totally different film junctions were realized based on two different types of hydrogen-bonding couplings. In particular, it was noticed that a stable but an imperfect multipoint hydrogen-bonding coupling was first built in the monolayer. This novel film architecture was realized as a result of a force balance of the strong hydrogen bonding between the two layers and the compression pressure. Of note is that the hydrogen-bonding force works in the direction of the surface perpendicular, whereas the compression pressure is in the surface-parallel direction. This study suggests that we would create novel film architectures if we could control the force balance between the two perpendicular forces. Because the compression pressure is an external force applied to the monolayer film, the force balance can easily be controlled.

Along this line, in the present study, a new monolayer architecture has been created with the use of hydrogen bonding

* To whom correspondence should be addressed. E-mail: t5hasega@cit.nihon-u.ac.jp. Fax: +81 47 474 2579.
† Nihon University.
‡ Kyoto University.
§ University of Miami.

10.1021/jp035997h CCC: $25.00
Published on Web 10/02/2003

by trans amide groups in a newly synthesized compound and the compression pressure via the surface-pressure control. The new film architecture has been characterized by the measurement of the surface pressure−area isotherm, followed by the analysis of infrared multiple-angle incidence resolution (MAIR[10−13]) spectra after the monolayer film was transferred onto a germanium substrate to form an LB film. MAIR spectroscopy has recently been developed by one of the authors.[10] The infrared MAIR spectroscopic technique is a powerful tool to evaluate the structural anisotropy in a thin layer, and it enables us to perform molecular orientation analysis quite easily with no optical parameters. The present paper is the first report of the unique monolayer film characterized by our new spectroscopic technique. The analytical results suggested that the new monolayer had a quite unique film architecture, which was consistent with all of the analytical results.

Material and Methods

The Rink amide resin and amino acid used for peptidolipid synthesis were purchased from Advanced Chem Tech (Louisville, KY). Other chemicals and solvents were purchased from Aldrich (St. Louis, MO) or Acros (Pittsburgh, PA) and used without further purification.

Synthesis of Peptidolipid. The peptidolipid was synthesized via standard solid phase 9-fluorenylmethoxycarbonyl (Fmoc) chemistry.[14,15] The amino acid Fmoc-Cys(Trt)-OH was used to construct the peptide backbone. A diisopropylcarbodiimide (DIC) and 1-hydroxylbenzotriazole (HOBt) in situ activation method was used for the coupling reactions. The Fmoc groups were de-protected with 20% piperidine solution in DMF. The hydrophobic long chain (C_{18}) was introduced by reacting stearic acid activated with DIC with the peptide. Cleavage of peptidolipid from the resin was conducted with the following cleavage cocktail: TFA (trifluoroacetic acid)/phenol/water/1,2-ethanedithiol; 82.5/5/5/2.5, v/v, the cleavage time is 2.5 h. After the synthesis, un-reacted TFA was removed by bubbling N_2. The crude products did not precipitate in diethyl ether, instead water was used for the precipitation. The crude product was lyophilized under vacuum. Semipreparative RP-HPLC was performed on a Waters 2690 separations module. A reversed-phase diphenyl column was used (219TP1010, Vydac Inc). Two solutions were prepared: A, 0.1% TFA in water and B, 0.1% TFA in 2-propanol/acetonitrile (1/1, v/v). A linear gradient (30∼70% B within 40 min, flow rate at 2 mL/min) was used.

Analysis of Peptidolipid. The purity of synthesized peptidolipid was characterized with analytical HPLC, ^{1}H NMR, and mass spectrometry. Analytical HPLC was conducted on a small-scale column (219TP5415, Vydac Inc). The same gradient as the semipreparative method was used (flow rate at 0.8 mL/min). ^{1}H NMR data was taken on Bruker 500 MHz spectrometers. Low resolution FAB was recorded on a VG-Trio 2000 mass spectrometer. High-resolution FAB was conducted on a 70-4F instrument in the Mass Spectrometry Lab, University of Illinois at Urbana−Champaign.^{1}H NMR (500 MHz, $CDCl_3$): $\delta = 4.77$ (2H, t), 3.05 (4H, m), 2.36 (2H, m), 1.80−1.60 (2H, m), 1.40−1.10 (28H, m), 0.86 (3H, t). FAB-MS: 490.3064 (MH^+, calcd 490.3059).

Surface Pressure−Area Isotherm Measurements. The peptidolipid compound (M_w = 489.79) was dissolved in chloroform at a concentration of 1.0 mg mL^{-1}, and 60 μL of the sample solution was spread on pure water maintained at 25 °C. The water was purified by a Millipore (Molsheim, France) Milli-Q Labo water purifier equipped with a micro filter (Millipak-40) having micropores of 0.22 μm to remove unexpected organic contaminants. The resistivity of the pure water was 18.3 MΩ cm, and the surface tension was 72.8 mN m^{-1} at 25 °C. Surface pressure−area (π−A) isotherms were measured by a Kyowa Interface Science (Saitama, Japan) HBM LB-film apparatus. The compression rate was 0.136 nm^2 min^{-1} molecule^{-1}. All of the π−A isotherms were measured at pH 5.8 of the pure water subphase.

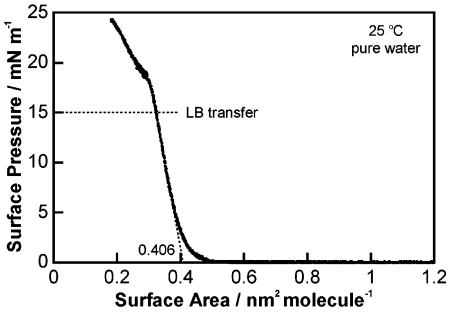

Figure 1. Surface pressure−area isotherm of the monolayer prepared on pure water at 25 °C.

Preparation of the Langmuir−Blodgett Film. The spread monolayer film on water was compressed up to 15.0 mN m^{-1} which corresponds to the solid state of the monolayer (Figure 1), and the single monolayer was transferred on a germanium (Ge) plate by the vertical dipping method.[16] The Ge plate was purchased from Pier Optics (Gunma, Japan) with a size of 40 × 20 × 1 mm (1 mm is the thickness). After cleaning the surface of the plate by a chemical rinsing,[13] the plate was used as the substrate of the LB film. The withdrawing rate of the substrate for the LB film deposition was 0.5 cm min^{-1}.

Infrared Spectroscopic Analysis. The FT-IR MAIRS measurements were performed by using a Harrick Scientific Co. (Ossining, NY) Brewster's angle sample holder (BXH−S1G). The angle of incidence was changed manually from 10° to 45° by 5° steps. This technique requires no polarizer.[10] The collection of infrared single-beam spectra was performed on a Nicolet (Madison, WI) Nexus 670 FT-IR spectrometer equipped with a mercury−cadmium−telluride (MCT) detector with an aperture fully opened.[11] The laser modulation frequencies for the interferogram collections were 60 kHz. The interferogram was accumulated 2000 times to improve the signal-to-noise ratio.

Because the measurements of MAIRS spectra are performed by collection of transmission single-beam spectra, the enhancement by the optical effect is not expected for the OP-mode spectrum, which is different from the RA measurements. Nevertheless, it is of note that LB films are deposited on both sides of the substrate, which earns double absorbance in comparison to the single-sided reflection measurements. Further, no requirement of a polarizer for the MAIRS analysis also contributes to high-sensitive measurements of thin films. Therefore, it is possible to analyze single-monolayer level LB films, although the signal-to-noise ratio is relatively poorer than the IP-mode spectrum.

Although the air in the sample room of the FT-IR was purged by dried air generated by an Airtech (Yokohama, Japan) AT-35H air-dryer, minute water vapor remained to be detected. Regardless, the residual water vapor does not have to do with the angle of incidence, and the signal intensity of the water vapor does not linearly respond to the **R** matrix (described later) in MAIRS. As a result, most of the water signals were discarded by the regression calculation. Water peaks that still remained particularly in the OP-mode spectra were readily corrected by subtraction of a water vapor spectrum.

CHART 1: Chemical Structure of the Newly Synthesized Peptidolipid Used in This Study

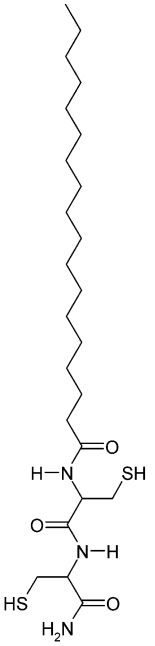

Results and Discussion

The newly synthesized peptidolipid (Chart 1) was spread on the water surface, and the $\pi-A$ isotherm was measured as presented in Figure 1. The isotherm lifts off at a surface pressure of zero at about 0.5 nm^2 $molecule^{-1}$, and the isotherm exhibits a straight line between 5 and 17 mN m^{-1}. Following compression to 15 mN m^{-1}, the film was decompressed to near zero pressure and then recompressed to 15 mN m^{-1}, almost an identical isotherm was reproduced, which suggested that the monolayer was not collapsed, and a stable monolayer was formed on water in this range of compression. When the monolayer was compressed more than 17 mN m^{-1}, however, the collapse of the monolayer was observed. Therefore, the linear part of the isotherm corresponds either to the solid state or the liquid-condensed state of the monolayer.

The limiting molecular area that represents the cross-section area of the molecule was analyzed from the linear part of the isotherm. As presented in Figure 1, the limiting molecular area is 0.41 nm^2 $molecule^{-1}$. This limiting molecular area is unexpectedly large for a single-chain molecule. It is known that the limiting molecular area for a single-chain molecule with a small-size headgroup is about 0.2 nm^2 $molecule^{-1}$, which is represented by normal alkanoic acid monolayers.[17] Although the hydrophilic group of the compound would have some steric effect, the molecular cross-section area would still be small as long as it is oriented perpendicularly to the surface, and therefore, the extraordinary large limiting molecular area cannot be explained simply by the size of the hydrophilic group. In other words, the large molecular cross-section suggests unusual molecular interdigitation or orientation of the head moiety in the monolayer.

To answer this question, the monolayer was transferred onto a Ge substrate, and it was subjected to FT-IR MAIRS analysis. MAIRS is a recently proposed new analytical technique, which enables us to simultaneously measure both in-plane (IP) and out-of-plane (OP) mode spectra of thin films deposited on a substrate. No technique other than MAIRS can measure pure OP-mode spectra on "nonmetallic" surfaces. The novelty of MAIRS has an impact on analysis of structural anisotropy in thin films, which has been performed by comparing the IP and OP-mode spectra thus far.[18] In other words, this technique indicates that the thin film architecture is unaffected by the substrate. In the present study, a monolayer that has unknown architecture and property is analyzed, which may be influenced by the contact with substrates. Therefore, the FT-IR MAIRS technique has been chosen to be the most suitable analytical tool.

In a conventional reflection−absorption (RA) technique, film samples are prepared on a metallic surface, and the infrared ray is oriented at a grazing angle of incidence. The incidental ray and reflected one are interacted with each other, which yields a strong electric field that has a perpendicular direction to the film surface. In this fashion, RA spectroscopy has the notable characteristic that perpendicular-oriented distribution of electric field is artificially generated near the metal surface, which gives the RA-specific surface selection rule.[18] the MAIRS technique, on the other hand, has a totally different optical concept.

In MAIRS, an infrared ray that has an electric field vector being parallel to the ray is virtually considered,[10] and the intensity of the transmitted ray ($\mathbf{s}_{obs}$) at an oblique angle of incidence is formulated by use of the intensities of the virtual ray ($\mathbf{s}_{OP}$) and the ordinary ray ($\mathbf{s}_{IP}$)

$$\mathbf{s}_{obs} = r_{IP}\mathbf{s}_{IP} + r_{OP}\mathbf{s}_{OP} \tag{1}$$

Here, r_{IP} and r_{OP} are mixing ratios for the linear combination. Because the spectral intensity has wavenumber dispersion, $\mathbf{s}_{obs}$, $\mathbf{s}_{OP}$, and $\mathbf{s}_{IP}$ are all vectors, and $\mathbf{s}_{obs}$ is collected as single-beam (not absorbance) spectra.[10] The mixing ratios are theoretically evaluated for various angles of incidence, and the series of equations are summarized in a matrix form as presented below:

$$\mathbf{S} \cong \begin{pmatrix} \mathbf{s}_{obs1} \\ \mathbf{s}_{obs2} \\ \cdot \\ \cdot \\ \cdot \end{pmatrix} = \begin{pmatrix} r_{IP1} & r_{OP1} \\ r_{IP2} & r_{OP2} \\ \cdot & \cdot \\ \cdot & \cdot \\ \cdot & \cdot \end{pmatrix} \begin{pmatrix} \mathbf{s}_{IP} \\ \mathbf{s}_{OP} \end{pmatrix} + \mathbf{E} \cong \mathbf{R} \begin{pmatrix} \mathbf{s}_{IP} \\ \mathbf{s}_{OP} \end{pmatrix} + \mathbf{E} \tag{2}$$

$$\mathrm{R} = \left(\frac{4}{\pi}\right)^2 \begin{pmatrix} 1+\cos^2\theta_j + \sin^2\theta_j \tan^2\theta_j & \tan^2\theta_j \\ \cdot & \cdot \\ \cdot & \cdot \end{pmatrix} \tag{3}$$

The subscript indicates different angles of incidence. Because the mixing ratios, **R**, are rigorously fixed via the theoretical evaluation, both $\mathbf{s}_{IP}$ and $\mathbf{s}_{OP}$ are precisely deduced by a regression calculation using the observed single-beam spectra matrix, **S**. The regression calculation obeys the classical least squares (CLS) regression as the following:[18−20]

$$\begin{pmatrix} \mathbf{s}_{IP} \\ \mathbf{s}_{OP} \end{pmatrix} = (\mathbf{R}^T\mathbf{R})^{-1}\mathbf{R}^T\mathbf{S} \tag{4}$$

The superscripts, T and −1, indicate transpose and inverse matrices, respectively. For the details of the evaluation of **R**, the reader is referred to literature.[10]

In our previous reports, the angles of incidence were chosen to be in the range of 5−45°. Nevertheless, after many observations, it has recently been found that 5° should be removed, because this small angle has a large experimental error due to the angular dispersion of the focal beam of infrared ray in the spectrometer. Therefore, in the present study, a new range of 10−45° was employed.

Figure 2 presents FT-IR MAIRS spectra of the peptidolipid single-monolayer LB film deposited on a Ge substrate. For the

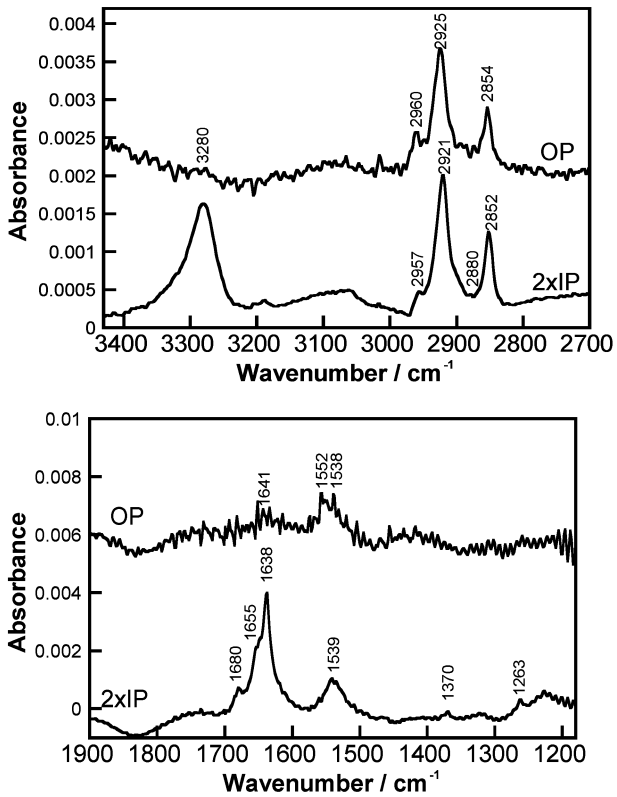

Figure 2. FT-IR MAIRS spectra of the LB film deposited on a germanium substrate. IP- and OP-mode spectra are both presented.

later molecular orientation analysis, the absorbance of the IP-mode spectrum is doubled.[10] The OP-mode spectrum is always obtained worse in signal-to-noise ratio than IP-mode for thin films of a single-monolayer level, because only the small component, $\tan^2\theta$, in the **R** matrix contributes to the retrieval of $\mathbf{s}_{OP}$ in the range of the angles. In the present results, however, it is of note that a useful OP-mode spectrum is yielded for a single-monolayer LB film on a nonmetallic surface.[22,23] At least, the spectra clearly show that the N−H stretching vibration (ν(N−H)) band at 3280 cm^{-1} and amide I band (mainly due to the C═O stretching vibration mode) at 1638 cm^{-1} have large band intensity ratios between the IP and OP-mode spectra. Discussion of band assignments will be mentioned in detail later. The large intensity ratios between the two-modes spectra strongly suggest that the N−H and C═O groups are highly oriented, and the directions of the groups should be near parallel to the film surface. As mentioned in previous literature, MAIRS spectra can be used for evaluation of molecular orientation by making a ratio of the IP and OP-mode spectral intensity as the following:[13]

$$\varphi = \tan^{-1}(\sqrt{2I_{IP}/I_{OP}}) \qquad (5)$$

The orientation angles of the ν(N−H) and amide I bands were calculated to be 86° and 85°, respectively, from the normal to the surface. The large orientation angles confirm the nearly parallel orientation to the film surface for the two bonds. Furthermore, almost the same orientation angles suggest that the N−H and C═O bonds are linearly aligned, which strongly supports that they are stably hydrogen bonded with each other, because hydrogen bonding is most stabilized when they are linearly lined.[4]

From these results, a schematic drawing is presented in Figure 3. We can consider that the spread molecules on water are associated one another via hydrogen bonding to form a specific molecular arrangement even at a low surface pressure before compression. Figure 3a shows such an interdigitated molecular arrangement at a surface pressure of zero. In this figure, it should be noted that the film molecules have three kinds of C═O groups: (1) the unassociated C═O group in a secondary amide, (2) the hydrogen bonded C═O group in the secondary amide, and (3) the hydrogen bonded C═O group in the primary amide (see Figure 3a). Because of the molecular structure, the C═O group at the connection part between the hydrocarbon chain and headgroup could not be hydrogen bonded, and it would remain an unassociated group. On the other hand, other two C═O groups would be associated via hydrogen bonding with N−H group in the interdigitated architecture.

Let us examine the interdigitation model by looking at amide I bands. In Figure 2, three amide I bands are found at 1639, 1655, and 1680 cm^{-1}. According to Nakanishi and Solomon,[22] three types of C═O groups at 1640, 1650, and 1680 cm^{-1} are respectively assigned to the associated primary and secondary amide I bands and unassociated secondary amide I band. These three modes correspond well to the three types of C═O groups in Figure 3a. By comparison of the band positions in the literature to our observations, the bands in the IP-mode spectrum at 1638 and 1655 cm^{-1} are respectively assigned to the hydrogen bonded primary and secondary amide I modes, whereas the band at 1680 cm^{-1} is assigned to the unassociated secondary amide I mode. If this model was correct, at least the C═O bonds in the secondary amide groups found at 1638 and 1655 cm^{-1} would be hydrogen bonded with the N−H bond in a neighbor molecule, which are expected to be oriented in the parallel direction to the film surface. This speculation is supported by the molecular orientation analysis as mentioned above. In this manner, as long as the ν(N−H) and amide I bands are analyzed, the model of molecular architecture presented in Figure 3a seems to be reasonable.

Another informative band is the amide II band. This mode is found at 1539 cm^{-1} in the IP-mode spectrum, whereas the same mode appears as doublet peaks at 1538 and 1552 cm^{-1} in the OP-mode spectrum, which are assigned to unassociated and hydrogen bonded amide II modes of the trans secondary amide, respectively.[22] If the hydrogen bonded C═O bonds are aligned in the parallel direction to the film surface as discussed for the I band, the hydrogen-bonded amide II mode should also be highly oriented. According to Miyazawa et al.,[25] the amide II mode comprises the C−N stretching vibration and the N−H bending vibration modes, and the contribution of the N−H bending is dominant. This requires that the transition moment of the amide II mode should be near perpendicular to the N−H bond. If the N−H bond had a parallel transition moment to the film surface as discussed earlier, therefore, the amide II mode would appear mainly in the OP-mode spectrum. As a matter of fact, the band at 1552 cm^{-1} attributed to the hydrogen-bonded amide II mode appears apparently in the OP-mode spectrum, whereas it appears weakly in the IP-mode spectrum. This suggests that the molecular model in Figure 3 and the analytical results of the amide II band are both correct.

The C−H stretching vibration region (2800−3000 cm^{-1}) is also useful for the discussion. In this region, the CH_2 symmetric and asymmetric stretching vibration bands ($\nu_s(CH_2)$ and $\nu_a(CH_2)$) are particularly notable. The band intensity ratios between the IP and OP-mode spectra are small (close to unity) for the two bands, which suggest that the hydrocarbon chain is not highly organized or it has a large tilt angle (see eq 5). Of more interest is, however, that the two bands appear at different wavenumber

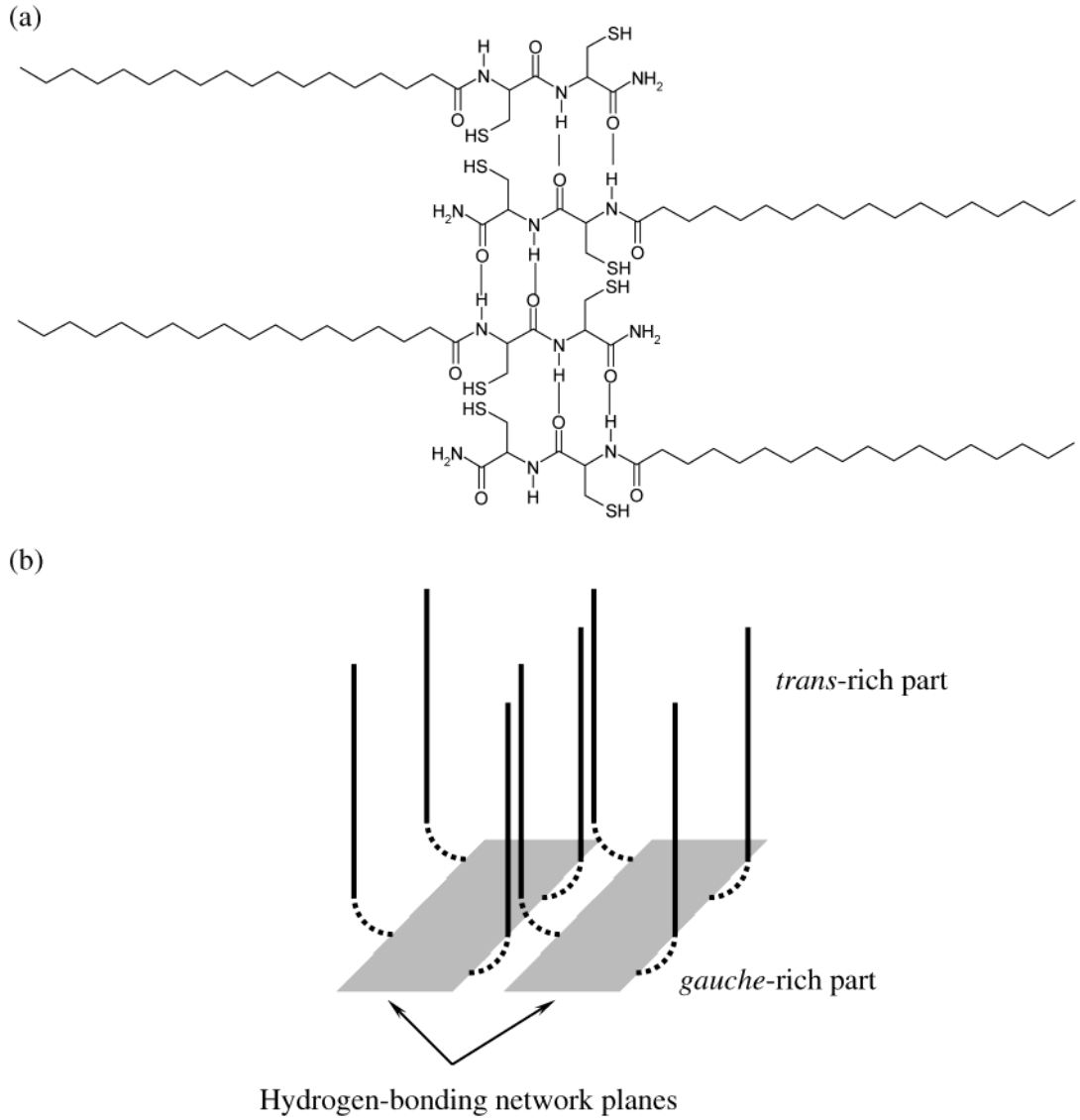

Figure 3. Estimated molecular film architecture on water at (a) a very low surface pressure and (b) in a monolayer in the liquid-condensed state.

positions for the IP and OP-mode spectra. The $\nu_a(CH_2)$ band, for example, appears at 2921 cm^{-1} in the IP-mode spectrum, whereas the same band appears at 2925 cm^{-1} in the OP-mode spectrum. It has already been reported that a large transition dipole such as the C═O bond sometimes results in the TO-LO splittings[22,26] that are observed in the IP and OP-mode (transmission and RA) spectra, which causes an apparent wavenumber shift between the two spectra. Nevertheless, the C−H stretching vibration bands are known to show no band shift because of the small transition dipole. Therefore, it is very interesting to find the band-location shift for both $\nu_s(CH_2)$ and $\nu_a(CH_2)$ bands.

This band shift is understandable when the molecular model in Figure 3b is taken into account. When the spread molecules on water shown in Figure 3a are compressed, the hydrocarbon chains would stand up, so that the limiting molecular area would decrease. Because the multipoint hydrogen-bonding network[5,8,9] is formed in the monolayer (Figure 3a), on the other hand, the monolayer stability would become large, and the planer hydrogen-bonding network is expected to remain stable on water as drawn in Figure 3b by the gray zone. As a result, the root part of the hydrocarbon chain would be bent. In other words, this molecular model is a result of a force balance between the molecular stabilization by crystal packing for the hydrocarbon chain and the hydrogen bonding formed among the interdigitated headgroups. To our best knowledge, the molecular architecture based on this mechanism has never been proposed.

If the molecular model shown in Figure 3b was correct, a further speculation can be made that the hydrocarbon chain would comprise two parts: trans- and gauche-rich parts. The trans-rich part is located near the end of the hydrocarbon chain, and it would contribute to the crystal stabilization in the monolayer. Although this part would be disordered to some extent due to the loose molecular packing after the interdigitation, the direction of the transition moments of the $\nu_s(CH_2)$ and $\nu_a(CH_2)$ modes would be nearly parallel to the surface. Therefore, the trans-rich part that yields low-wavenumber bands would contribute to the IP-mode spectra mainly.

On the other hand, the gauche-rich part is considered to be located at the root part of the hydrocarbon chain. Because this is a connection part between the surface-parallel (hydrogen bonded headgroup plane) and surface-normal (trans-rich hydrocarbon chain) parts, the gauche-rich part would have molecular stress and disorder in comparison to the trans-rich part. Another important characteristic of the gauche-rich part is that the $\nu_s(CH_2)$ and $\nu_a(CH_2)$ modes would contribute not only to the IP-mode spectrum, but also to the OP-mode one because of the molecular bending. As a result, the gauche-rich part that would

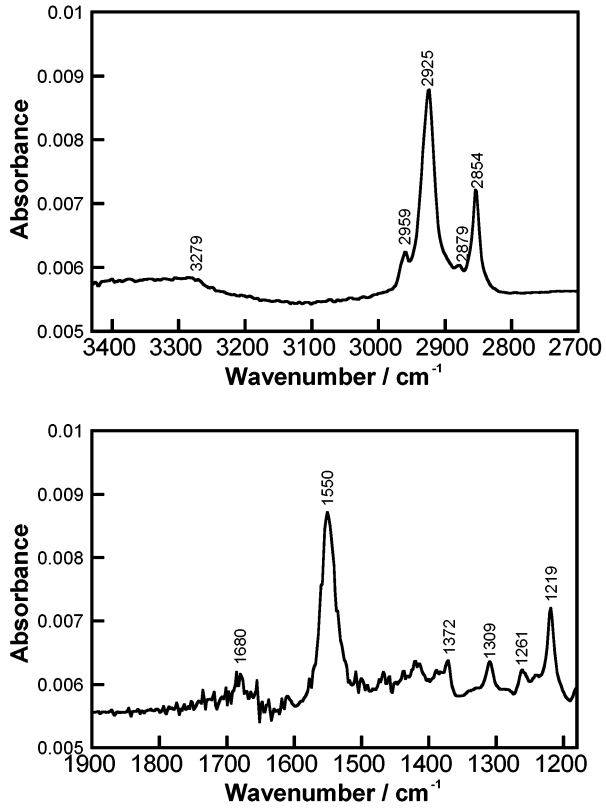

Figure 4. Infrared reflection−absorption spectrum of the monolayer LB film, which corresponds to that used for Figure 3.

yield higher wavenumber bands than the trans-rich part is expected to appear in the OP-mode spectrum strongly.

This discussion made on the molecular model in Figure 3b is reasonable to understand the band shift between the IP- and OP-mode spectra. It is concluded that the shift is not caused by an optical effect like the TO-LO splitting but by the unusual molecular bending in the film. The bending model is consistent with the large tilt angle of the hydrocarbon chain suggested by the small band-intensity ratio of the CH_2 stretching vibration bands. Further, this interdigitation model is also reasonable to account for the large limiting molecular area. As found in Figure 3b, this film-architecture model requires about double the molecular space in the film. This speculation is quite consistent with the observed limiting molecular area (0.41 nm^2 $molecule^{-1}$).

In this manner, the $\pi-A$ isotherm and the FT-IR MAIRS spectra are reasonably elucidated. Regardless, the estimated molecular model is too unusual to accept naturally. This model was then reexamined by RA spectroscopy.

The molecule in the present study has two thiol groups that are not reacted with other molecules. If the model in Figure 3b would be correct, the thiol groups would be oriented nearly parallel to the film surface. When the monolayer is transferred onto a gold-evaporated glass slide, the thiol groups would react with the gold surface to form covalent Au−S bonds. In other words, if the film-architecture model would be correct, the film architecture would be fixed by making the Au−S covalent bonds, and almost the same spectrum as the OP-mode spectrum would appear in the RA spectrum.

Figure 4 presents an infrared RA spectrum of the single-monolayer LB film deposited on a gold-evaporated glass slide transferred at 15.0 mN m^{-1}. The spectral pattern is quite similar to the OP-mode spectrum by FT-IR MAIRS. In particular, the high wavenumber regions resemble each other: the wavenumber positions are perfectly reproduced by the RA spectrum, and the relative intensity of the C−H and N−H bands are also reproduced. We tried to transfer the same monolayer on a "silver"-evaporated glass slide, but the transfer ratio was very poor (ca. 0.1), and the RA spectral pattern (data not shown) was largely different from Figure 4. This means that the analysis of this monolayer depends on the substrate, and the analytical technique using a common substrate for both IP and OP-mode spectra is useful. The consistency of the RA spectrum to the MAIRS OP-mode spectrum strongly suggests that the molecular model in Figure 3b is reasonable. The relative intensity of the amide II band (1550 cm^{-1}) to the C−H stretching vibration bands is also reproduced well by the RA spectrum. In the OP-mode spectrum of FT-IR MAIRS, the amide II band has a comparative band intensity to the $\nu_s(CH_2)$ band after taking the absorbance scale into account. This intensity relation is also recognized in the RA spectrum. The amide I bands in the RA spectrum are, on the other hand, almost invisible except for the band at 1680 cm^{-1}. As mentioned above, the band at 1680 cm^{-1} is assigned to the unassociated C═O bond at the root of the hydrocarbon chain. This suggests that the associated C═O groups with the N−H group via hydrogen bonding are oriented to the surface parallel, whereas only the unassociated C═O group would have the surface-normal component of the transition moment.

Conclusion

On a new concept of molecular film construction by use of surface pressure as well as molecular interactive forces, a novel monolayer architecture has been built, which has been analyzed by a new spectroscopic technique: infrared MAIRS on Ge. The extraordinary larger than expected limiting molecular area was readily elucidated by the molecular model that was suggested by the MAIRS spectra. The OP-mode spectrum of the MAIRS spectra was confirmed to be correct by performing infrared RA spectroscopic measurements for the transferred monolayer on a gold-evaporated glass slide. The fixed monolayer by forming the covalent Au−S bonds has more organized film architecture than that deposited on a Ge substrate. Therefore, the molecular model suggested by MAIRS has been confirmed by the infrared RA analysis.

The present result suggests that the force balance using an external force to the monolayer would be a useful concept to develop a new film architecture without making covalent bonds among the film molecules.

Acknowledgment. This work was financially supported by Cooperative Research Projects under the Japan−U.S. Cooperative Science Program co-organized by Japan Society for the Promotion of Science and the National Science Foundation (U.S.A.), and by Grant-in-Aid for Scientific Research for Priority Areas "Dynamic Control of Strongly Correlated Soft Materials" (No. 413/14045267) and Exploratory Research (No. 15659011) from the Ministry of Education, Science, Sports, Culture, and Technology, Japan.

References and Notes

(1) Becher, P. *Dictionary of Colloid and Surface Science*; Marcel Dekker: New York, 1990.

(2) Gaines, G. L. *Insoluble Monolayers at Liquid−Gas Interface*; Interscience: New York, 1966.

(3) Skvarla, J. V. *Adv. Colloid Interface Sci.* **2001**, *91*, 335.

(4) Jeffrey, G. A. *An Introduction to Hydrogen Bonding*; Oxford: New York, 1997.

(5) Hasegawa, T.; Hatada, Y.; Nishijo, J.; Umemura, J.; Huo, Q.; Leblanc, R. M. *J. Phys. Chem. B* **1999**, *103*, 7705.

(6) Huo, Q.; Sui, G.; Zheng, Y.; Kele, P.; Hasegawa, T.; Nishijo, J.; Umemura, J.; Leblanc, R. M. *Chem. Eur. J.* **2001**, *7*, 4796.

(7) Huo, Q.; Russev, S.; Hasegawa, T.; Nishijo, J.; Umemura, J.; Puccetti, G.; Russel, L. C.; Leblanc, R. M. *J. Am. Chem. Soc*. **2000**, *122*, 7890.

(8) Ahuja, R.; Caruso, P.-L.; Möbius, D.; Paulus, W.; Ringsdorf, H.; Wildburg, G. *Angew. Chem., Int. Ed. Engl.* **1993**, *32*, 1033.

(9) Koyano, H.; Bissel, P.; Yoshihara, K.; Ariga, K.; Kunitake, T. *Chem. Eur. J.* **1997**, *3* 1077.

(10) Hasegawa, T. *J. Phys. Chem. B* **2002**, *106*, 4112.

(11) Hasegawa, T.; Matsumoto, L.; Kitamura, S.; Amino, S.; Katada, S.; Nishijo, J. *Anal. Chem.* **2002**, *74*, 6049.

(12) Hasegawa, T. *Anal. Bioanal. Chem.* **2003**, *375*, 18.

(13) Hasegawa, T.; Matsumoto, L.; Kitamura, S.; Amino, S.; Katada, S.; Nishijo, J. *Can. J. Anal. Sci. Spectrosc.* **2003**, *48*, 157.

(14) Fields, G. B.; Noble, R. L. *Int. J. Pept. Protein Res*. **1990**, *35*, 161.

(15) Stewart, J. M. In *Method Enzymology*; Fields, G. B., Ed.; Academic Press: New York, 1997; Vol. 289, pp 44−67.

(16) Blodgett, K. B. *J. Am. Chem. Soc*. **1934**, *56*, 495.

(17) Gericke, A.; Hühnerfuss, H. *J. Phys. Chem. B* **1993**, *97*, 12899.

(18) Umemura, J. *Reflection−Absorption Spectroscopy of Thin Films on Metallic Substrates*. In *Handbook of Vibrational Spectroscopy vol. 2*; Chalmers, J. M., Griffiths, P. R., Eds.; John Wiley: Chichester, U.K., 2002; pp 982−998.

(19) Hasegawa, T. *Principal Component Regression and Partial Least Squares Modeling vol. 3*; Chalmers, J. M., Griffiths, P. R., Eds.; John Wiley: Chichester, U.K., 2002; pp 2293−2312.

(20) Kramer, R. *Chemometric Techniques for Quantitative Analysis*; Marcel Dekker: New York, 1998.

(21) Massart, D. L.; Vandeginste, B. G. M.; Buydens, L. M. C.; de Jong, S.; Lewi P. J.; Smeyers-Verbeke, J. *Handbook of Chemometrics and Qualimetrics Parts A and B*; Elsevier Science, Amsterdam, 1997.

(22) Hasegawa, T.; Takeda, S.; Kawaguchi, A.; Umemura, J. *Langmuir* **1995**, *11*, 1236.

(23) Hasegawa, T.; Nishijo, J.; Umemura, J.; Theiβ, W. *J. Phys. Chem. B* **2001**, *105*, 11178.

(24) Nakanishi, K.; Solomon, P. H. *Infrared Absorption Spectroscopy*, Emerson Adams: New York, 1962.

(25) Miyazawa, T.; Shimanouchi, T.; Mizushima, S. *J. Chem. Phys.* **1958**, *29*, 611.

(26) Yamamoto, K.; Ishida, H. *Vib. Spectrosc.* **1994**, *8*, 1.